Available online at www.sciencedirect.com
ScienceDirect
International Journal of Heat and Mass Transfer 51 (2008) 344–352
International Journal of HEAT and MASS TRANSFER
www.elsevier.com/locate/ijhmt

Effects of pore size distribution and pore-architecture assembly on drying characteristics of pore networks

Somkiat Prachayawarakorn [a,*], Preeda Prakotmak [b], Somchart Soponronnarit [b]

[a] Faculty of Engineering, King Mongkut's University of Technology Thonburi, Suksawat 48 Road, Bangkok 10140, Thailand
[b] School of Energy and Materials, King Mongkut's University of Technology Thonburi, Suksawat 48 Road, Bangkok 10140, Thailand

Received 6 March 2006
Available online 20 September 2007

Abstract

Simulation of isothermal drying using two-dimensional networks comprised of interconnected cylindrical pores is presented. Transport of moisture inside pore segments was described by Fick's law. The results have shown that the shielding of large pores by the smaller pores in the stochastic pore network, which is supposed to be representative of real porous medium, causes the lower drying rate and hence lower effective diffusion coefficient as compared to those predicted from the idealized network of pores with a single size. The strength of shielding is found to vary with the characteristics of pore size distribution as interpreted by the moisture concentration experienced by the pores, which is remarkably different amongst the pore size distributions. The inefficient transport of moisture through the stochastic pore network can be improved or even better with the suitable architecturally assembled structure. The minimum shielding archetype network, appearing very high porous at particle surface, is predicted to enhance greatly the drying rate. On the other hand, the maximum shielding network, which is small pores allocated onto the network exterior, exhibits the slowest drying rate.

Keywords: Drying; Effective diffusion coefficient; Stochastic pore network

1. Introduction

Drying of porous materials has received much attention in a number of industrial applications including wood [1], pharmaceutical product [2], foodstuffs [3], and paper [4]. While material is dried, moisture inside the material transports through its interfacial void spaces to the surface and is carried away to the flowing stream. The transport of moisture may be occurred by several mechanisms of mass transfer, such as Knudsen diffusion, molecular diffusion, capillary flow, etc. All the drying mechanisms are lumped into the effective (apparent) diffusion coefficient [5–7] and the porous material is considered as a continuum. This consideration leads to formulation of partial differential equations which relate to the changes of quantities, i.e. temperature and moisture content with time. By using the continuum models, the effective diffusion coefficient can experimentally be determined from the drying characteristic curve. The value of the effective diffusion coefficient varies from material to material although the drying conditions used, i.e. temperature and superficial air velocity, are all the same. The summary of the effective diffusion coefficients for products are given by [8]. However, the interpretation of those results have ignored the pore structural issues and relied on empirical representations. Such empiricisms may not be useful for providing detailed information on how moisture diffuses through void spaces, with different sizes and shapes, which dictate the diffusive pathways of moisture.

Thus, it is desirable to obtain the structural models that are capable of taking into accounts key geometrical and topological properties such as dead ends and variations in pore size and tortuous trajectories. When the structural model is combined with the transport equations, the flow

* Corresponding author. Tel.: +662 4270 9221; fax: +662 428 3534.
E-mail address: somkiat.pra@kmutt.ac.th (S. Prachayawarakorn).

0017-9310/$ - see front matter © 2007 Elsevier Ltd. All rights reserved.
doi:10.1016/j.ijheatmasstransfer.2007.03.055

Nomenclature

C	moisture content (decimal dry basis)
$\overline{C}$	average moisture content (decimal dry basis)
D	diffusion coefficient (m^2/s)
Fo	Fourier number, $\frac{D\Delta t}{\Delta x^2}$
N	drying rate, kg water/s, or number of pores in network
Pr	probability distribution function
L	material thickness (m)
l	pore length (m)
r	pore radius (m)
t	drying time (s)
x	distance along the pore length (m)

Greek symbols

σ	standard deviation (m)
μ	mean pore radius (m)
Γ	gamma function
κ	adjustable parameter of uniform distribution
ψ	adjustable parameter of uniform distribution
α	adjustable parameter of bimodal distribution
β	adjustable parameter of bimodal distribution

Subscripts

e	equilibrium
eff	effective

of substances through pore segments inside porous solid can numerically be predicted [9–11] and hence the effective properties are calculated, thereby providing the understanding of macroscopic properties. In such a way, network models can be used in the modeling of transport processes such as single-phase and two-phase fluid flow and pore diffusion [12–15].

In this work, the drying of the random or stochastic pore network, which is supposed to be representative of pore spaces of real porous particle, is investigated. The moisture movement inside the pore segments is described by Fick's law and the drying process occurs under isothermal condition. The effect of pore size distributions on the drying characteristic curve and subsequent effective diffusivity is theoretically determined. In addition to the pore size distribution, the geometrical configuration of the pores, which is a full set of pores assembled in different ways onto the network, is explored how the diffusion of moisture through such geometrical structure exhibits different to that predicted from the stochastic pore network. This geometrical structure, sometimes called as pore architecture in this work, has similar pore size distribution to that employed in the stochastic pore network.

2. Network model

Fig. 1 shows an example of scanning electron micrograph (SEM) views of dried durian chip obtained from the freeze and hot air dryings. Pores shown in Fig. 1 are represented by black color and tissue by grey color. Porosity of the material appears to consist of a randomised assembly of pore spaces, which are more or less randomly interconnected. As shown from the figure, different drying techniques can produce remarkably different microstructures. Durian chip dried by the freeze-drying technique is more porous and larger pore sizes than that dried by hot air. With the hot air dried sample, the dense layer is formed and the small pores appear at the surface.

To understand the transport of moisture through the pore spaces, the pore sizes of the real solid is mapped onto an array of lattices (shown in 2-D in Fig. 2). Each pore in the real solid becomes a bond in one of the lattices and each pore junction becomes a node. In this study, the pore shape assigned onto the network is assumed to be cylindrical geometry and all pores in the network are assumed to have

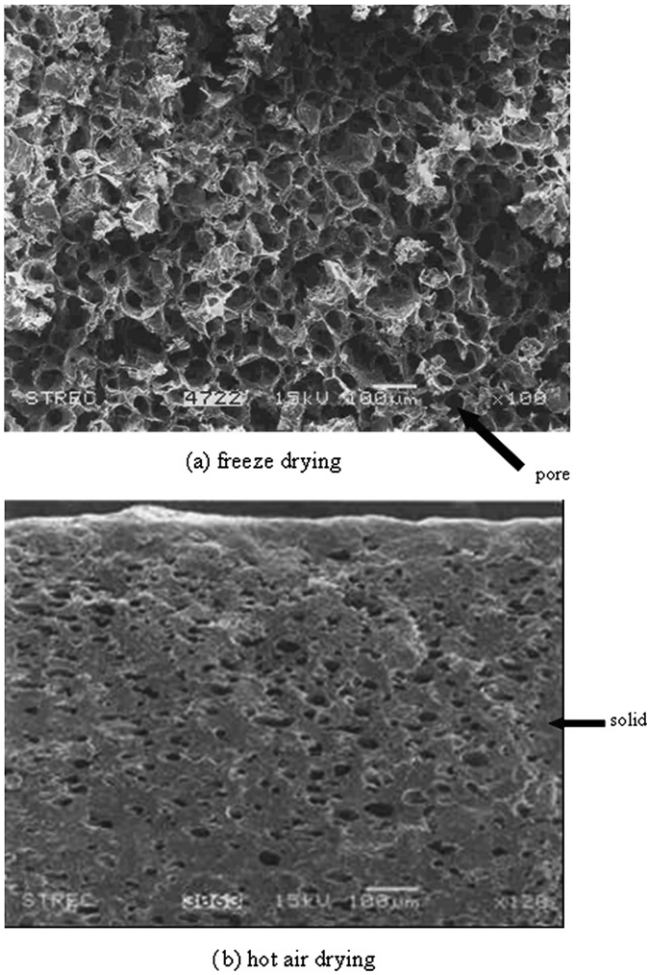

(a) freeze drying

(b) hot air drying

Fig. 1. SEM images of durian chip obtained from different drying techniques.

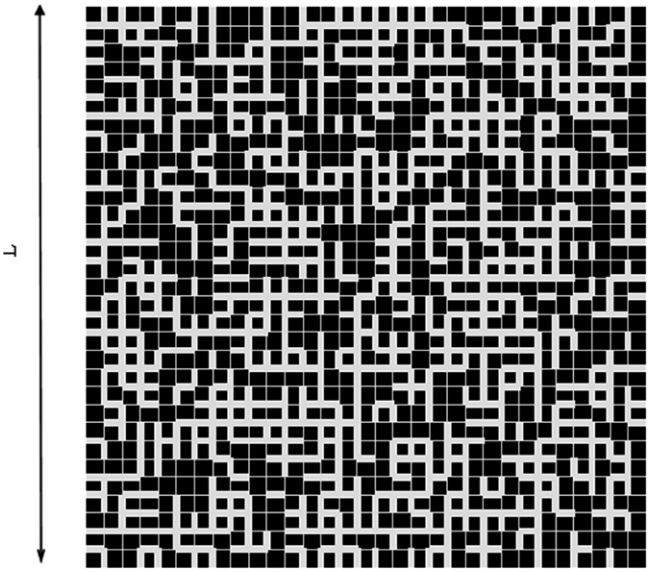

Fig. 2. 2-D 30 × 30 random pore network.

the same length. The pores with different sizes are randomly placed onto the network and this approach provides pore at any positions within the network independent to the neighboring pores. Fig. 2 illustrates 2-D pore network with a size of 30 × 30, consisting of 1860 pores. Each pore junction has a connectivity of 4. Real pore sizes of solid, which may determined by nitrogen adsorption or mercury porosimetry, are assigned to the bonds so that the real structure and the network model have the same pore size distribution. Let L is the average particle size of material. The length of each pore, l, is then calculated by dividing L by $N+1$, where N is the network size. Moisture leaves from the network via all the pores at the network periphery, which open onto the drying medium.

2.1. Diffusion in single pores

When the pore network is established, the diffusion problem is solved by calculating the moisture content inside the individual pore in conjunction with the mass balance of moisture at the pore junctions. It is assumed that the moisture diffusing through pore with radius $r_{i,j}$, occurs under isothermal condition. The isothermal condition occurs when heat required for evaporation balances with heat from conduction and convection. The change of moisture inside individual pores of the network is described by the following equation:

$$\frac{\partial C}{\partial t} = D\frac{\partial^2 C}{\partial x^2} \tag{1}$$

where C is the moisture content (decimal dry basis), D the diffusion coefficient (m^2/s), t the drying time (s) and x the distance along the pore length (m). The diffusion coefficient is assumed to be a constant value and the moisture concentration in the pores at the beginning is specially uniform along the pore axis. To determine the moisture profile along the length, the forward finite difference is applied and Eq. (1) is thus expressed as

$$C^{p+1}_{m,r_{i,j}} = Fo\left(C^{p}_{m-1,r_{i,j}} + C^{p}_{m+1,r_{i,j}}\right) + (1-2Fo)C^{p}_{m,r_{i,j}} \tag{2}$$

where Fo is the Fourier number, $Fo = \frac{D\Delta t}{\Delta x^2}$, p and m the respective indexes of the present drying time and of nodal position along the pore. Eq. (2) is stable when Fo ranges between 0 and 0.5. The transfer rate $N_{i,j}$ of moisture, for any time t, diffusing into a pore with radius of $r_{i,j}$ can be calculated by

$$N_{r_{i,j}} = \pi r^2_{i,j} D\left(\frac{\mathrm{d}C_{r_{i,j}}(x,t)}{\mathrm{d}x}\right)_{x=l}. \tag{3}$$

2.2. Mass balance in the network

After drying starts, the pore ends positioned at the exterior network are exposed to the drying medium and have moisture equal to equilibrium moisture content, assuming negligible convective mass transfer resistance. This assumption allows the moisture contents of the exterior pores at any drying time to be calculated directly. For the interior pores, the calculation of their moisture contents is not straightforward since the moisture contents at the two ends of pore is not known. To determine the internal moisture contents, the mass balance of moisture content at inner nodes of the network is made, assuming the size of pore junctions being zero and no accumulation at the pore junctions within the network. The sum of all in and outflows, for a small time interval, at any node is accordingly zero. That is,

$$\sum_{j\in\{i\}} N_{r_{i,j}} = 0 \tag{4}$$

where $\{i\}$ refers to the set of i-adjacent nodes which are connected to node (i) in the network. By solving the moisture in every node together the specified boundary conditions around the network periphery, the average moisture content $\overline{C}_{\text{network}}$ of the network can readily be calculated. The calculation, based on the volume average, can be expressed by

$$\overline{C}(t)_{\text{network}} = \frac{\sum_{n=1}^{N} r^2_{i,j}\int_0^l C_{r_{i,j}}(x,t)\,\mathrm{d}x}{N\cdot l\sum_{n=1}^{N} r^2_{i,j}} \tag{5}$$

where N is the number of pore in the network and l is the pore length (m).

2.3. Effective diffusivity

If the diffusion is occurring through the slab-shaped porous solids, the effective diffusivity can be determined by Fick's second law of diffusion, which is expressed by

$$\frac{\overline{C}(t)-C_e}{C_i-C_e} = \frac{8}{\pi^2}\sum_{n=0}^{\infty}\frac{1}{(2n+1)^2}\exp\left[-(2n+1)^2\frac{\pi^2 D_{\text{eff}}t}{L^2}\right] \tag{6}$$

where $\overline{C}(t)$ is the average moisture content of material (decimal dry basis), C_i the initial moisture content, C_e the equilibrium moisture content, D_{eff} the effective diffusion coefficient and L the material thickness. Eq. (6) presents the diffusion of moisture in one direction. The drying of pore network at the present study is, however, occurred in two directions and the solution is obtained from the product of the above diffusion equation itself, thus eventually yielding

$$\frac{\overline{C}(t)-C_e}{C_i-C_e}=\left(\frac{8}{\pi^2}\right)^2\left[\exp\left(-2\pi^2\frac{D_{eff}\times t}{L^2}\right)+\left(\frac{2}{9}\right)\exp\left(-10\pi^2\frac{D_{eff}\times t}{L^2}\right)+\left(\frac{2}{25}\right)\exp\left(-26\pi^2\frac{D_{eff}\times t}{L^2}\right)+\cdots\right] \quad (7)$$

The first three terms of infinite series of Eq. (7) are employed to quantify the effective diffusivity and a trial-error method is used. The effective diffusivity is obtained when the difference between the value of moisture content predicted by Eq. (7), $\overline{C}(t)$, and that calculated from the network, $\overline{C}(t)_{network}$, is less than the acceptable value. By this method, the evolution of moisture content at pore level directly reflects on the effective diffusivity.

2.4. Pore size distribution

Pore size distribution defined in the range from a minimum to a maximum pore radius, r_{min} and r_{max}, is described in terms of the number diameter probability density function which is given by

$$f(r)=\frac{d\left(\frac{N(r)}{N_T}\right)}{dr},\quad r_{min}<r<r_{max} \quad (8)$$

where N_T is the total pores in the network and $N(r)$ presents the number of pores between r and $r+dr$. The integration of Eq. (8) from r_{min} to r_{max} equals to unity, $\int_{r_{min}}^{r_{max}} f(r)\,dr=1$. The probability distribution function of all pores in the network with radius larger than a particular radius, $Pr(r_i)$, is

$$Pr(r_i)=\int_{r_i}^{r_{max}} f(r)\,dr \quad (9)$$

The values of $Pr(r_i=r_{min})=1$ and of $Pr(r_i=r_{max})=0$. In this study, the following three types of pore size distribution, i.e. normal distribution, uniform distribution and bimodal distribution were used:

Normal size distribution:

$$f(r)=\frac{1}{\sigma\sqrt{2\pi}}\exp\left(-\frac{1}{2}\left[\frac{r-\mu}{\sigma}\right]\right),\quad -\infty<r<\infty \quad (10)$$

Uniform size distribution:

$$f(r)=\frac{1}{\kappa-\psi},\quad \psi\leqslant r\leqslant\kappa \quad (11)$$

Bimodal size distribution:

$$f(r)=\frac{r^{\alpha_1-1}}{\Gamma(\alpha_1)\beta_1^{\alpha_1}}\exp\left(-\frac{r}{\beta_1}\right)+\frac{r^{\alpha_2-1}}{\Gamma(\alpha_2)\beta_2^{\alpha_1}}\exp\left(-\frac{r}{\beta_2}\right),\quad 0\leqslant r\leqslant\infty \quad (12)$$

where σ is the standard deviation, μ the mean pore radius, $\Gamma(\alpha)$ the gamma function and κ, ψ and α all the adjustable parameter.

Before investigating the diffusive flow behaviour within the network of pores, pore sizes are generated by the mapping of a sequence of uniformly distributed numbers in the range of 0 and 1 on the corresponding probability distribution function $Pr(r_i)$ and then are randomly distributed to the bonds.

3. Results and discussion

Drying simulations were performed on the pore network model. At the beginning, every pore within the network is assumed to have equal moisture content, with the value of 0.35 dry basis. When the drying starts, moisture content at the periphery pores immediately equilibrates to the surrounding air, which is assumed to be 0.165 dry basis in this study. The diffusivity value used in the simulations was 1×10^{-10} m^2/s. To minimize the effect of periphery pores on the transport of moisture, size of the network should sufficiently be large. In addition, it enables to capture the moisture transport inside the large network closed to that occurring inside the real porous materials, consisting of many thousands of pores. A network size of 45×45, consisting of 4140 pores in the network, was used in this study. For each set of results reported, 20–30 realisations were carried out and the average value was presented.

3.1. Influence of pore size distribution width

Pore size distribution is the important parameter not only in quality of foods but also in transport of moisture [16]. Their structures are given by a nature or through processing. To simplify the problem, this work assumes that the structure of foods does not change with time. Two case studies were performed; the first deals with the width of pore size distribution and the latter deals with the influence of characteristics of pore size distribution (see Section 3.2).

In the first case, the simulations were performed with the normal size distribution to determine the effect of pore size distribution width on the average moisture content. The width of distribution can be made by varying the value of standard deviation. A mean pore radius was given, with a size of 40 μm. The average moisture contents of the networks versus time are plotted in Fig. 3 for the values of standard deviation (σ) of 1, 7, and 12 μm. The moisture content of the network, for a given standard deviation, is rapidly decreased at the early drying period and slowly decreased afterwards. This trend is generally found in drying curve of porous materials.

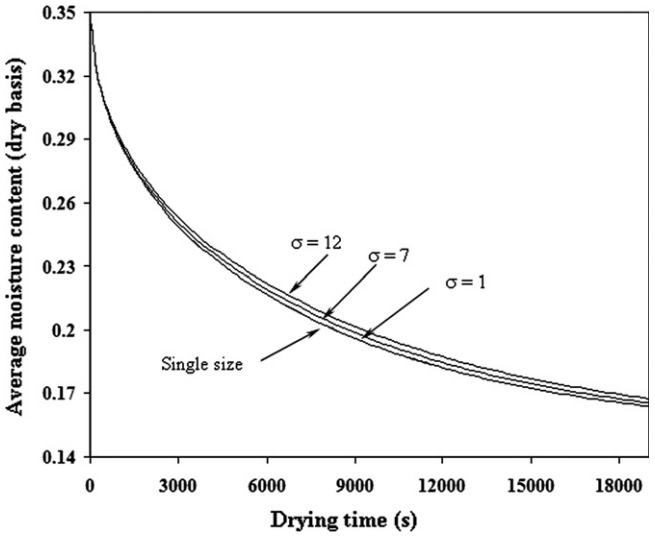

Fig. 3. Influence of pore size distribution width on moisture content (normal size distribution with $\mu = 40$ μm).

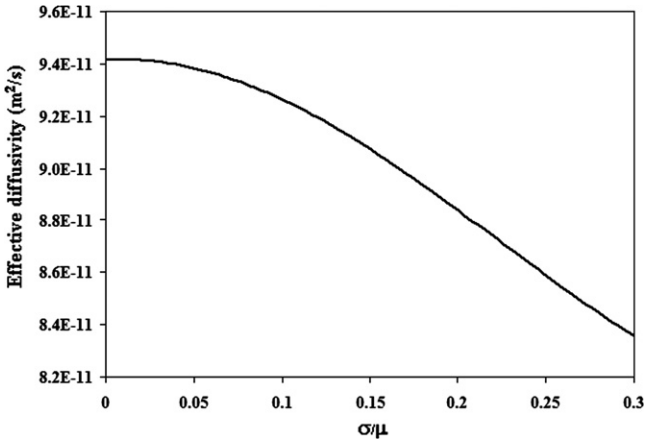

Fig. 4. Influence of pore size distribution width on transport property ($\mu = 40$ μm).

As shown in Fig. 3, difference in drying rate amongst pore size distribution widths is clearly evident after which moisture content of the networks is reduced below 0.25 dry basis. The moisture content is reduced faster with the narrower pore size distribution, corresponding to smaller standard deviation. When the standard deviation becomes unity, the decrease of moisture content is almost identical to that of the network of single-sized pore. The single-sized network is an ideal network where the moisture diffusing through any pore in the network is not interfered by their adjacent pores. These simulation results emphasize the less efficient transport of moisture within the network consisting of large and small pores, which are randomly connected. The poor transport is due to the larger pores shifted behind smaller ones and this effect is named as pore "shielding" [17]. Such shielding results in the moisture existing in the shielded pores difficult to move from the interior to the exterior because of the strong diffusional resistances in the surrounding pores.

However, the pore shielding effect is insignificant at the early drying period since the main portion of moisture removed at this time is present near the network periphery in which the moisture movement is not interfered by the disorder of void spaces within the network. Thus, the reduction of moisture content with time is nearly the same for the networks of pores that possess different standard deviations of pore size, as shown in Fig. 3.

The influence of the pore size distribution width on the drying curve presented in Fig. 3 is similar to that reported by Metzger and Tsotsas [18], exhibiting the strong effect of standard deviation of pore sizes on the drying behaviour. In their model, voids in porous material were represented as cylindrical shape and their arrangement was in parallel direction to fluid flow. The parallel capillaries were connected all along their length with no any resistance and fluid present in the capillaries was transported by the capillary and viscous forces. However, Segura and Toledo [19], who studied the isothermal drying of pore networks by assuming the dominant contribution of capillary forces over the viscous forces, reported the opposite results to the above studies. In their work, the simulation showed an insignificant effect of pore size distribution on the drying curves of the pore networks.

Fig. 4 shows the influence of width of pore size distribution on the effective diffusivity with a mean value of 40 μm. The effective diffusivity of the network reduces as the value of σ/μ increases. The value of effective diffusivity decreases from 9.4×10^{-11} m^2/s at the σ/μ of zero to 8.3×10^{-11} m^2/s at the σ/μ of 0.3. These results respond to the similar way found in the drying curves, showing the faster drying rate with lower value of standard deviation.

3.2. Influence of type of pore size distribution

In this section, the change in moisture transport, while it diffuses through the network with different distributive pores, i.e. uniform, normal and bimodal distribution, is studied. In comparison, the networks of pores, which are characterized by different types of pore size distribution, have equal total pore volume and the network length is equal. The structural parameters required to generate pore size distributions are given as follows:

Normal size distribution: $\mu = 40$ μm and $\sigma = 10$ μm
Uniform distribution: $\kappa = 74.13$ μm and $\psi = 4.97$ μm
Bimodal distribution: $\beta_1 = 3$ μm, $\beta_2 = 10$ μm, $\alpha_1 = 2$ μm and $\alpha_2 = 4.9$ μm

For the single-sized network, which is used as a baseline, the pore size of 40 μm was employed. Fig. 5 shows the number diameter probability density function of pores generated from different types of pore size distributions using the above structural parameters. In the bimodal distribution, the pore sizes are generally characterized by two groups, small and large pores. Pore sizes produced from

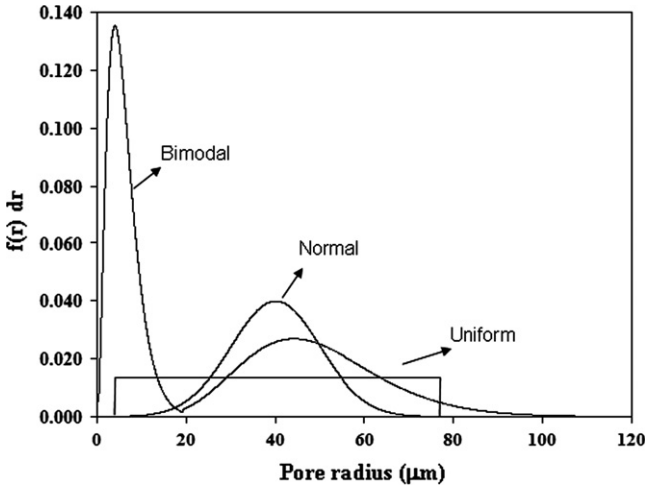

Fig. 5. Number diameter probability density function generated from different types of pore size distribution under the same total pore volume.

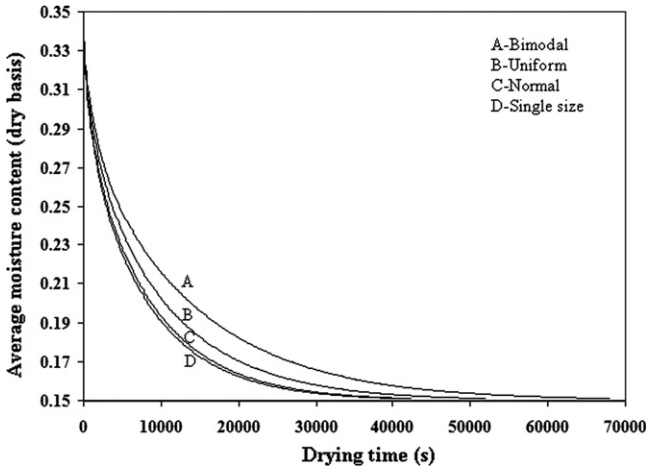

Fig. 6. Influence of type of pore size distribution on moisture content.

the structural bimodal parameters were given in the range of small pores from 0.34 to 17.3 μm, accounting for 36% of total number of pores allocated onto the network, and in the range of large from 17.3 to 121.8 μm, accounting for 64% of total number of pores. For the uniform distribution, the generated pore sizes ranged between 1.9 and 71 μm.

Fig. 6 shows the influence of type of pore size distribution on reduction in moisture content, indicating the strong impact of pore size distribution on the moisture change.

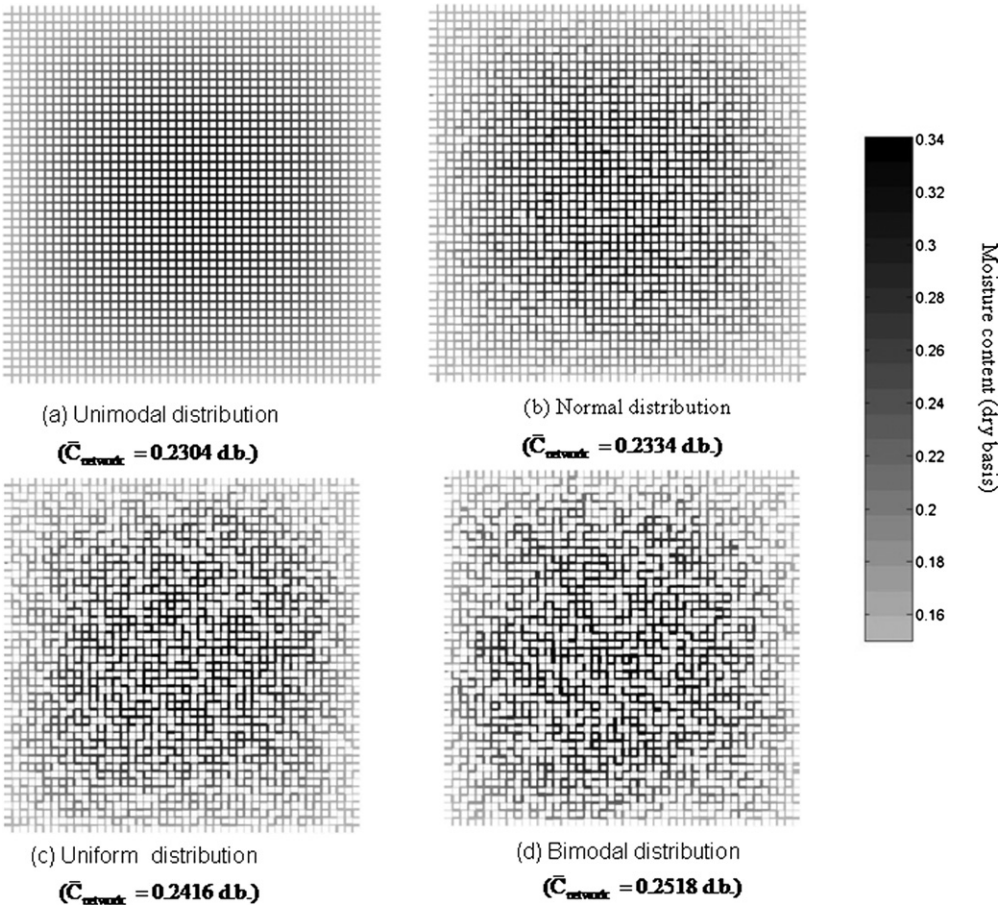

Fig. 7. Moisture content in 2-D pore networks with different distributions of pore sizes.

The rate of moisture reduction is lowest with the bimodal distribution and it becomes faster with the following uniform and normal distributions. Moreover, the fastest rate of moisture reduction exhibits in the single-sized network for which the shielded pores are absent. The moisture transport through the bimodal network is least efficient in spite of the larger pore sizes and higher pore volume in the large pore assembly, both of which normally serve high flow of moisture because of low resistance of moisture diffusion in the large pores. However, the slowest drying rate for the bimodal pores can be attributed to the fact that the large pore assembly ineffectively communicates itself throughout the network and some of them possibly allocate behind the smaller pores. Thus, the moisture diffusion from the inside to the outside for this pore size distribution is strictly limited. This description can be interpreted through the representation of network moisture gradients in voids which will be shown in Fig. 7.

The changes of average moisture content of the networks, with different pore size distributions, shown in Fig. 6 are selected for a particular drying time of 4500 s to visualize the moisture content of each pore positioned within the networks. The pictorialized representations of local moisture content are shown in Fig. 7. Each pore was colored according its moisture content. The representative colors with 21 shades from light grey to black were used for the corresponding range of moisture content from less than 0.16–0.34 dry basis. After drying is passed, difference in the detailed moisture contents amongst the networks of pores is shown up. As shown in Fig. 7d for the "bimodal" network, the inefficient connection of large and small pore assemblies exhibits the delay of moisture in percolating through the network once the drying front approaches the smaller pores. Irregular pattern of moisture content is also found with the bimodally distributed pores.

The results from the simulations also indicate that the moisture at the innermost pores of the "bimodal" network for the illustrative drying time of 4500 s is the same content as at the initial one (black), implying that drying at that area does not commences. With the other networks, the moisture at the innermost had already decreased, reducing from 0.34 to 0.32 dry basis which corresponds to the dark grey color.

3.3. Effect of structure re-ordering on the drying kinetics

The food materials in particular fruit possess dense physical structure and sugar content. When it is conventionally dried, the crust or dense layer may possibly be formed near the material surface. This created structure does not facilitate internal moisture movement, thus resulting in long drying time, browning and darkening of product and large energy consumption. One approach to improve the drying rate is to change its physical structure, for example, making it more porous. This can be made by the foaming of fruit before drying [20]. In this section, the concept of pore network is utilised to show how the drying rate can be changed when the physical structure of material is modified. Two illustrative structures are given to show the scope for this.

The first structure is shown in Fig. 8a whereby the full set of random pores, generated from the normal distribution ($\sigma = 10$ μm and $\mu = 40$ μm), is assembled in rank order and then spirally wound into positions in the network, with the largest pore at the exterior and the smallest at the centre. This architectural structure, namely minimum shielding network, exhibits very more porous at the exterior

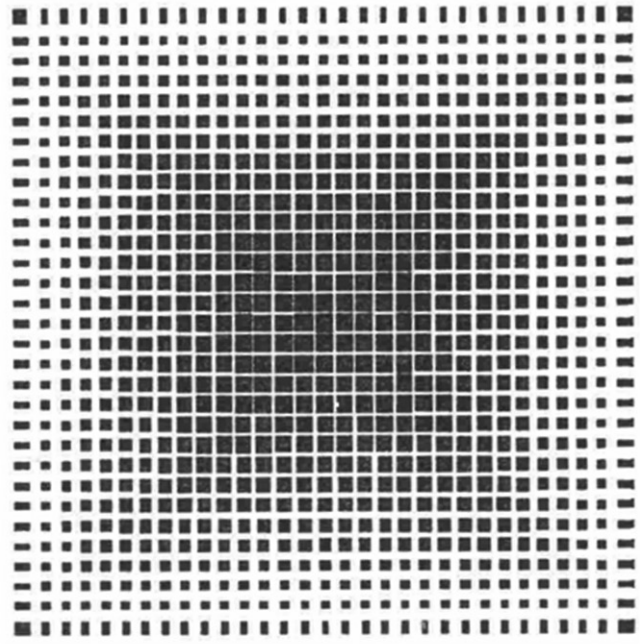

(a) minimum shielding network

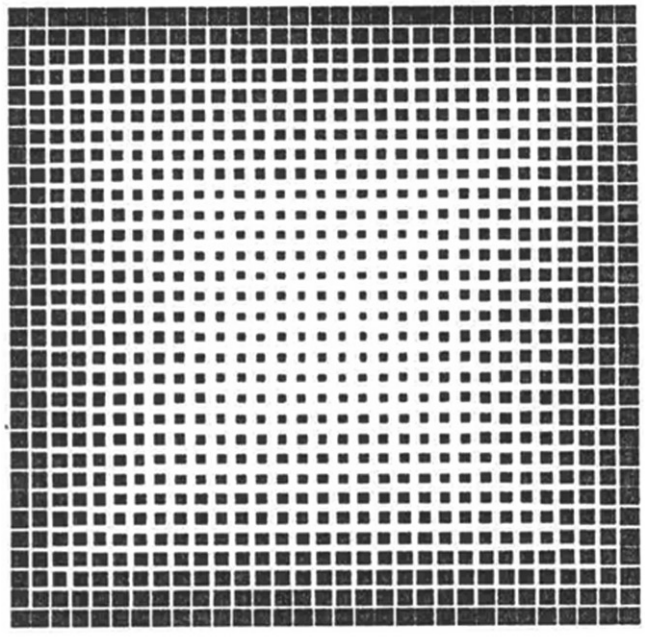

(b) maximum shielding network

Fig. 8. Illustrative pore architectural structures.

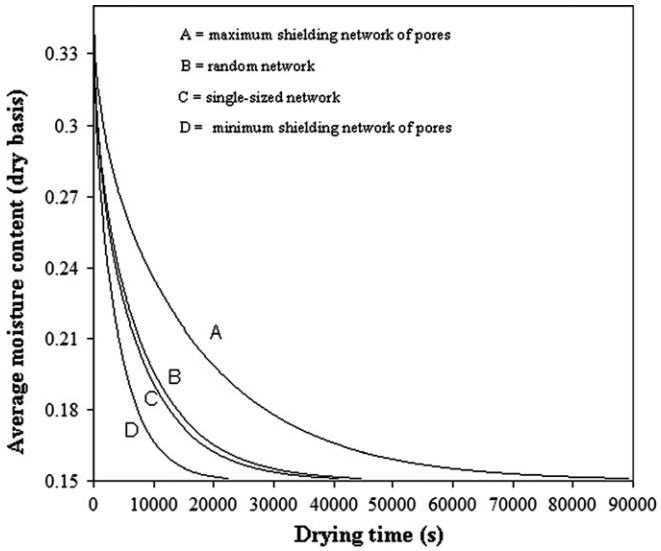

Fig. 9. Effect of pore architectural structure on the drying kinetics.

surface as shown in Fig. 8a. On the other hand, if the pores are allocated into the network, with the smallest size at the exterior surface and the largest at the centre, it can be visualized as a dense layer at the surface, which is shown in Fig. 8b, which is named as maximum shielding network. The outer dense layer of the later pore structure may possibly be similar to that occurring in the biomaterials containing high sugar content when dried with hot air. Both pore structures shown in Fig. 8 have exactly identical pore sizes used in the stochastic pore network. The simulation results obtained from the above archetypal pore structures are shown in Fig. 9. The transport of moisture through different configurations of pore assembly is strikingly different. The reduction of moisture content is very fast with the pore structure appearing very porous at the exterior (D) and extremely slowest with the dense structure at the exterior (A). The corresponding effective diffusivities are 1.57×10^{-10} m^2/s and 3.81×10^{-11} m^2/s.

The moisture content of each pore for the architectural configurations is shown in Fig. 10, for the illustrative drying time of 4500 s which is the same time as presented in Fig. 7. As shown in Fig. 10a for the minimum shielding network, the moisture content of the exterior pores at that time lies in between 0.16 and 0.2 dry basis, corresponding to the shade of grey color which increases intensity from light to medium grey. This result implies the architectural pore structure with very high porous at the outer surface facilitating the high diffusive flux of moisture, thereby enhancing the rapid fall in moisture content.

Because of high resistance of moisture diffusion in the small pores at the periphery for the maximum shielding network, the diffusion of moisture is restricted and this is clearly evident from Fig. 8b, showing the grey color shade only at the periphery pores whilst most inner pores have moisture contents above 0.3 dry basis.

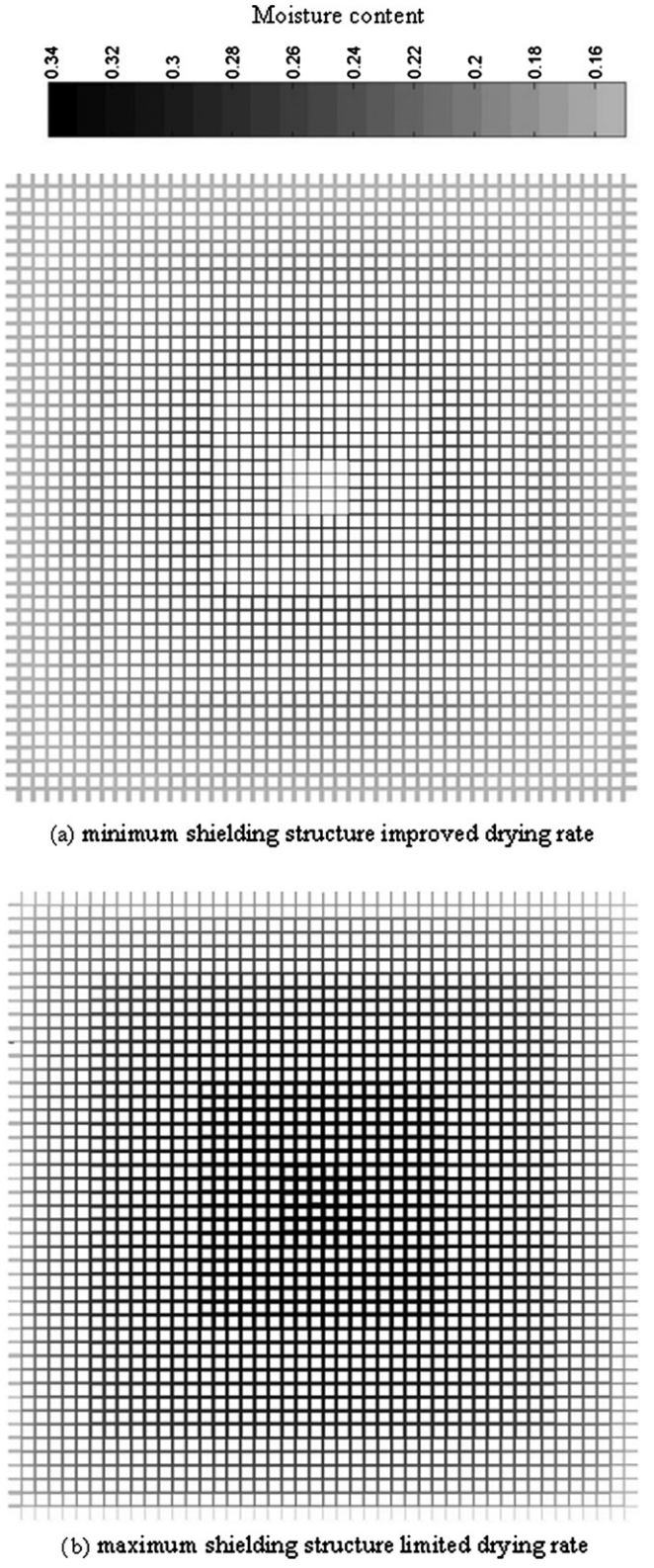

Fig. 10. Moisture content in 2-D network with different arrangements of pore assembly.

4. Conclusions

A 2-D pore network for the drying of moisture content under isothermal condition has been studied. The transport

of moisture within individual pore segments is described by Fick's second law. The simulation results have been shown that the effect of shielding inherent in typical random pore network results in slower decrease of moisture content and hence lower value of effective diffusion coefficient as compared to the single sized network for which the shielding is absent. Degree of shielding is different among pore size distributions and this effect causes the value of effective diffusion coefficient to be dependent on the distribution types. The strongest shielding effect is found with the pore network characterized by bimodal pore size distribution and this influence consequently results in drying of bidisperse porous structure relatively longer time than the other illustrative pore size distributions, i.e. uniform and normal distribution. The drying rate of the stochastic pore network can be improved through the proper pore structure. This superiority is greatest with the network of pores appearing highly porous at the exterior. On the other hand, porous particles, with a dense layer at the surface or consisting of small exterior pores, can be dried with lowest rate.

Acknowledgements

The authors express their sincere appreciation to the Thailand Research Fund and commission on higher education for financial support.

References

[1] D. Elustondo, S. Avramidis, S. Shida, Predicting thermal efficiency in timber radio frequency vacuum drying, Dry. Technol. 22 (2004) 795–807.
[2] K.H. Gan, R. Bruttini, O.K. Crosser, A.I. Liapis, Freeze-drying of pharmaceuticals in vials on trays: effects of drying chamber wall temperature and tray side on lyophilization performance, Int. J. Heat Mass Transfer 48 (2005) 1675–1687.
[3] L.A. Campañone, V.O. Salvadori, R.H. Mascheroni, Food freezing with simultaneous surface dehydration: approximate prediction of freezing time, Int. J. Heat Mass Transfer 48 (2005) 1205–1213.
[4] J. Seyed-Yagoobi, H. Noboa, Drying of uncoated paper with gas-fired infrared emitters – optimum emitters' location within a paper machine drying section, Dry. Technol. 21 (2003) 1897–1908.
[5] G. Efremov, T. Kudra, Calculation of the effective diffusion coefficients by applying a quasi-stationary equation for drying kinetics, Dry. Technol. 22 (2004) 2273–2279.
[6] Md. Raisul Islam, J.C. Ho, A.S. Mujumdar, Convective drying with time-varying heat input: simulation results, Dry. Technol. 21 (2003) 1333–1356.
[7] S. Prachayawarakorn, P. Prachayawasin, S. Soponronnarit, Effective diffusivity and kinetics of urease inactivation and color change during processing of soybeans with superheated-steam fluidized bed, Dry. Technol. 22 (2004) 2095–2118.
[8] N.P. Zogzas, Z.B. Maroulis, D. Marinos-Kouris, Moisture diffusivity data compilation in foodstuffs, Dry. Technol. 14 (1996) 2225–2253.
[9] M. Blunt, Flow in porous media-pore – network models and multiphase flow, Curr. Opin. Colloid Interface Sci. 6 (2001) 197–207.
[10] R. Mann, Development in chemical reaction engineering: issues relating to particle pore structures and porous materials, Trans. IchemE 71A (1993) 551–561.
[11] M. Sahimi, G.R. Gavalas, T.T. Tsotsis, Statistical and continuum models of fluid–solid reactions in porous media, Chem. Eng. Sci. 45 (1990) 1442–1502.
[12] S.C. Nowicki, H.T. Davis, L.E. Scriven, Microscopic determination of transport parameters in drying porous media, Dry. Technol. 10 (1992) 925–946.
[13] J.B. Laurindo, M. Prat, Numerical and experimental network study of evaporation in capillary porous meida. Drying rates, Chem. Eng. Sci. 53 (1998) 2257–2269.
[14] M. Prat, Isothermal drying of non-hygroscopic capillary-porous materials as an inversion percolation process, J. Multiphase Flow 21 (1995) 875–892.
[15] V.G. Mata, J.C.B. Lopes, M.M. Dias, Porous media characterization using mercury porosimetry simulation. 1. Description of the simulator and its sensitivity to model parameters, Ind. Eng. Chem. Res. 40 (2001) 3511–3522.
[16] M.S. Rahman, O. Al-Amri, I.M. Al-Bulushi, Pores and physico-chemical characteristics of dried tuna produced by different methods of drying, J. Food Eng. 53 (2002) 301–313.
[17] G.P. Androutsopoulos, R. Mann, Evaluation of mercury porosimeter experiments using a network pore structure model, Chem. Eng. Sci. 34 (1979) 1203–1212.
[18] T. Metzger, E. Tsotsas, Influence of pore size distribution on drying kinetics: a simple capillary model, Dry. Technol. 23 (2005) 1797–1809.
[19] L. Segura, P.G. Toledo, Pore-level modeling of isothermal drying of pore networks: effects of gravity and pore shape and size distributions on saturation and transport parameters, Chem. Eng. J. 111 (2005) 237–252.
[20] C.K. Sanket, F. Castaigne, Foaming and drying behaviour of ripe bananas, Lebensm-Wiss. Univ. Technol. 37 (2004) 517–525.